Indian Geotechnical Journal, 38(4), 2008, 454-482

Soil-Structure Interaction Analysis of a Braced Deep Excavation

Rajendra Karki[*] and Jitendra S. Sharma[**]

Introduction

Over the past few decades, several factors have led to an increase in the number of people migrating to large cities. Consequently, these large cities are getting overpopulated because of the limitations in lateral expansion. Quite expectedly, the land required for residential and business purposes is getting increasingly scarce, necessitating the creation of space by building vertically or in 'tiers' – both upwards and downwards – to maximize the land use. Deep excavations, often in congested urban settings, are increasingly becoming a common sight because of such vertical expansion of the cities.

There are two main issues associated with deep excavations in an urban environment: (1) the design and construction of adequate temporary support system for the deep excavation; and, (2) the prevention or minimization of damaging effects of deep excavation on adjacent structures and their foundations. Engineers responsible for such deep excavation often struggle finding answers to several pertinent questions such as:

- How can the risk of damage to the adjacent properties be minimized during a deep excavation?
- Is it safe to carry out the excavation with the existing condition of the site?
- What are the methodologies that are best suited to monitor and control the effects of a deep excavation?
- What may be the limiting criteria to stop the work in case of impending failure?

Typically, the engineer responsible for the design of a support system for a deep excavation tries to develop a numerical model of the excavation using sophisticated non-linear finite element software and tries to incorporate all aspects of the soil-structure interaction into the numerical model. However, such a numerical model is both highly complex and data deficient, and therefore, its findings cannot be implemented with full confidence. It is, therefore, common to use the Observational Method (Peck 1969a) for such projects. In the

[*] Geotechnical Engineer, Leighton Group Inc., Irvine, California, USA

[**] Department of Civil & Geological Engineering, University of Saskatchewan, 57 Campus Drive, Saskatoon SK S7N 5A9 CANADA, Tel: +1 306 966-7049, Fax: +1 306 966-5427 (shared), E-mail: J. Sharma@usask.ca

Observational Method, the construction is started using initial analysis and design done using the best possible estimates of ground condition and input parameters. Worst case design scenarios are also established using the most unfavourable ground conditions and input parameters, which are used to set trigger values for unacceptable performance and early warning of incipient failure. One of the key components of the Observational Method is the on-site instrumentation to monitor and evaluate the performance during construction. If monitoring data show a below par performance, the design is revised and contingency measures based on revised design are implemented. The success of the on-site instrumentation program, however, depends upon the identification and understanding of key soil-structure interaction mechanisms.

The complexity of the soil-structure interaction mechanisms of a deep excavation in the midst of existing structures is well-known. Various components such as support system, surrounding ground, foundations of existing structures, buried structures such as tunnels and underground caverns interact with each other during excavation. The following factors that influence this interaction have been identified (Peck 1969b; Mana and Clough 1981; Peck 1985; Wong and Broms 1989; Clough and O'Rourke 1990; Athanasiu et al. 1991; Hashash and Whittle 1996; Burd et al. 2000):

> Stiffness and strength characteristics of the surrounding soil such as anisotropy, rate effects, nonlinearity, and hysteretic behaviour.

> Pore-water pressure changes and accompanying consolidation of the surrounding soil

> The type and the stiffness of the support system

> Behaviour of interface between the soil and the structure

> Type of the foundation for adjacent structures

> Stiffness of the lining system in case of adjacent buried structures

> The location (horizontal distance as well as the depth of cover) of adjacent structures

> The sequence of excavation and the quality of workmanship

Given the wide scope of this soil-structure interaction problem as evident from the above-mentioned factors, it is not surprising that key aspects of this problem are not yet fully understood and there exists a strong need to do further research in this area.

This paper begins with a brief overview of the use of the finite element method in the study of soil-structure interaction. Details and results of finite element back-analysis of an instrumented deep excavation in an urban setting are then presented and discussed. The finite element analysis software PLAXIS (Brinkgreve et al. 2004) was used for the back-analysis. In the finite element back-analysis, both non-linear elastic and elastoplastic models were used to describe the various soil layers and key aspects of the construction, such as sequential excavation of layers, installation of pre-stressed tie-back anchors and props and dewatering of the excavation, were modelled. Input parameters were first calibrated using the back analysis and then used for establishing the key mechanisms of soil-structure interaction. The findings of the finite

element back-analysis are further extended using the results of a parametric study that was conducted to identify the key parameters that influence the mechanisms of soil-structure interaction.

Background

The use of the finite element method to analyze geotechnical problems started in 1970s with the advent of digital computing and advances made in terms of analytical and numerical techniques. With the availability of affordable computing power and improved constitutive models of soil behaviour, its use has increased exponentially and its status has changed from luxury to necessity. Now-a-days, it is hard to imagine geotechnical analysis and design being done without using the finite element method.

Three main applications of the finite element method to deep excavation can be found in published literature:

- For design calculations and prediction of ground movements and structural forces;
- For back-analysis of existing case histories; and
- For conducting parametric studies.

When used for design calculations and prediction of ground movements and structural forces, the finite element method usually forms an important component of the Observational Method. Also, back-analyses of case histories using the finite element method are often accompanied by parametric studies. A few of the notable uses of the finite element method in the analysis and design of deep excavations are presented in the subsequent paragraphs. Palmer and Kenney (1972) used the finite element method to evaluate the relative importance of different parameters on the performance of a braced excavation at Oslo Subway in Norway. Of the parameters concerning soil condition, the soil deformation modulus was found to have the greatest influence. Other important parameters affecting the deflection of retaining wall were the stiffness of sheet-pile wall and effective strut stiffness.

Burland and Hancock (1977) described the performance of the multi-propped excavation in sand and gravel overlying stiff, fissured London clay and reported that approximately 50% of the total ground movements (both horizontal and vertical) occurred due to the construction of the diaphragm wall and piles. Eisenstein and Medeiros (1983) reported the performance and analysis of a deep excavation in glacial till and found that the flexibility of the retaining wall has a significant effect on lateral pressure reduction and on ground movements. The total horizontal load carried by the struts and by the embedded portion of the wall was also found to depend on wall flexibility.

Finno and Harahap (1991) used parametric studies using the finite element method to demonstrate the importance of sheet pile installation and other construction factors on ground movements around a deep excavation. The finite element simulations closely modelled all phases of construction including sheet-pile installation and the actual duration of construction. While sheet-pile deflections could be accurately estimated for all the stages of the excavation, the estimatd ground movement diverged from the observed response after the

onset of yielding followed by localized straining of soil. Powrie and Li (1991) used finite element analyses to study the complex soil-structure interaction between the retaining wall, the soil and a continuous slab propped at the formation level of a 9-m-deep excavation in stiff over-consolidated boulder clay. It was found that computed deformations were governed by the assumed stiffness of the soil rather than the flexural rigidity of the wall. Bending moments in the wall were influenced significantly by the assumed pre-excavation lateral earth pressures and, to a lesser extent, by the nature of the structural connection between the wall and the permanent prop slab.

Ng and Lings (2002) evaluated the effectiveness of two relatively simple models: a linear elastic-perfectly plastic Mohr-Coulomb and a nonlinear BRICK model (Simpson 1992) for simulating the top-down construction of a multi-propped excavation in the over-consolidated stiff fissured clay. The results of the study show that the use of a Mohr-Coulomb model with a 'wished-in-place' simulation of wall installation can reasonably predict the maximum bending moments and deflections of the wall for design purposes once the input soil parameters are correctly estimated. However, it significantly overestimates strut loads and fails to estimate the general ground deformation pattern.

Long (2001) used the finite element method to back-analyze the case history of a deep basement excavation in London Clay. Parametric studies on the effect of various parameters indicated that "best estimates" of the wall movements were still well in excess of those measured. It was concluded that these differences were due to three-dimensional effects and deficiencies in the constitutive modelling of soil behaviour. Moormann and Katzenback (2002) studied three-dimensional effects of a 13-m-deep excavation in soft clay. The excavation was rectangular in plan view. The results showed that a plain strain model overestimates the horizontal displacements of the wall and the settlements at the ground surface as well as the internal forces of the side of the wall and of the supporting system. Calvello and Finno (2004) used the finite element method to perform inverse analysis of an instrumented deep excavation supported by props and tie-back anchors to calibrate the input parameters for the soil. It was shown that the use of calibrated input parameters resulted in better estimates of the horizontal deformation of the retaining wall.

From the overview of the use of finite element method in the analysis and design of deep excavations, it can be seen that there is no general agreement between the results obtained by various researchers. It is evident that more research is needed to achieve a better understanding of the soil-structure interaction mechanisms that are at play in and around a deep excavation. In the next section, such mechanisms are explored with the help of finite element back-analysis of a well-documented case history of a deep excavation in clay supported by a combination of diaphragm walls, props and tie-back anchors.

Details of the Case Study

The case study selected for the finite element back-analysis is a deep excavation in downtown Chicago for the Chicago Subway Renovation Project (Finno et al. 2002; Calvello and Finno 2004). This particular case study was selected because of the availability (in public domain) of reliable data on local geology, soil properties, and lateral deformation of the retaining wall during

installation as well as during excavation. The deep excavation involved the installation of a braced stiff excavation support system for the rehabilitation of a metro subway station (Finno et al. 2002). The rehabilitation included partial demolition of the existing dual subway tunnel tube and expansion of the subway station. A 12-m deep excavation was carried out in soft-to-medium glacial clay. The excavation was supported by a 900-mm-thick secant pile wall, one level of cross-lot bracing (struts) and two levels of tiebacks as shown in Figure 1.

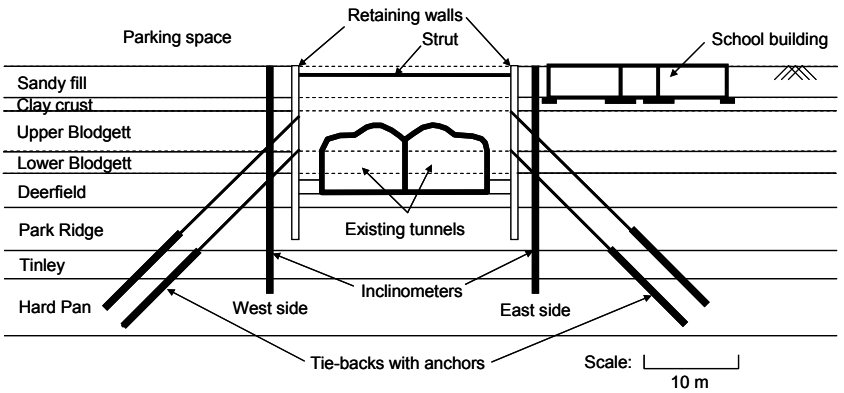

Fig. 1 Section View of Excavation Support – Chicago Subway Renovation Project (Adapted from Calvello and Finno, 2004)

The deep excavation was challenging and risky due to the presence of a school building in the vicinity. The school was founded on shallow foundations located within 1.3 m of the wall of the excavation. The bracing and anchoring support system was carefully designed to minimize the damage to the adjacent school. As expected in the planning phase, some minor damage occurred to non-load bearing portions of the school building. Out of 28 mm of horizontal movement, 10 mm occurred during wall installation and 18 mm occurred during deep excavation as shown in Figure 2 (Finno et al. 2002).

The site consists of a fill deposit overlying a sequence of glacial clays deposited during the Pleistocene period (figure 1). The fill is mostly medium dense sand with construction debris in some parts. Beneath the fill lie four glacial clays, namely Upper and Lower Blodgett, Deerfield, and Park Ridge. With the exception of a clay crust in the upper portion of the Blodgett stratum, these deposits are lightly overconsolidated as a result of lowering groundwater levels after deposition and/or aging (Calvello 2002). The Blodgett stratum consists of a desiccated crust and underlying soft clays with undrained shear strengths that increase with depth. This stratum is supraglacial in origin and is characterized by a relatively wide range of water contents and liquid limits. The Deerfield stratum consists of medium stiff clay and is characterized by uniform water contents. The Park Ridge stratum is a stiff to very stiff clay with lower water contents than the Deerfield stratum. Below the four glacial clays is the Tinley stratum, which consists of very stiff to hard clay and silts. The hard soils are encountered at around 18 m depth and are locally known as ‘Hard Pan’ (Roboski 2001; Calvello 2002).

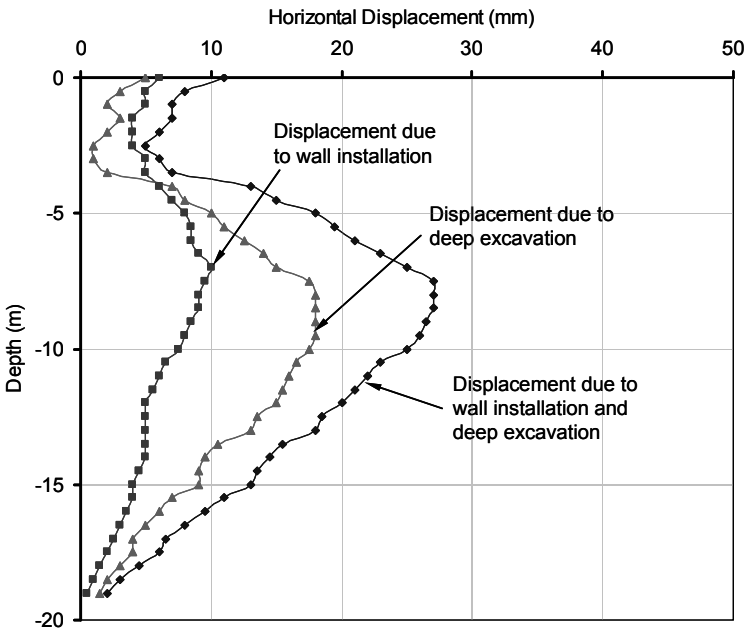

Fig. 2 Chicago Subway Renovation Project - Observed Horizontal Displacement of the Retaining Wall (Based on the Data Contained in Finno et al. 2002)

Finite Element Back-analysis

Assumptions

The following assumptions were made to achieve simplification of the modelling of deep excavation:

> All the deformations are assumed to occur in a plane strain condition even though the length to width ratio of the excavation was only 1.6.

> The geometry of the cross-section shown in Figure 1 is assumed to be symmetric about a vertical axis that passes through the web separating the two subway tunnels. In order to save on computational time, only the left half of the cross-section is modelled in PLAXIS. Strictly speaking, the cross-section is not symmetric because of the presence of the raft foundation for the school on the east side of the excavation (Figure 1); however, incorporation the raft foundation for the school in the model would have added unnecessary complexity to the model. It should, therefore, be noted that the results of the back analyses are not applicable to the east side of the cross-section.

> The effect of the construction of the subway tunnel on the surrounding ground is not modelled. The deformations due to tunnel construction are nullified by resetting the displacements to zero.

> The complex cross-section of the tunnel is replaced by a simple box cross-section.

> The retaining wall is modelled as 'wished-in-place', i.e. the unloading of the ground during the installation of secant pile wall is not modelled.

> Seepage analysis to establish ground water flow condition is not incorporated in the model. It is unlikely that there would be any significant ground water flow from the surrounding ground into the deep excavation because the soil layers near the base of the excavation have fairly low permeability values and their behaviour is likely to be undrained during excavation. It should be pointed out that when seepage analysis is not incorporated in a PLAXIS model of deep excavation, the pore water pressures on either side of the retaining wall are considered equal as shown in Figure 3(a). By default, a submerged excavation is, therefore, simulated. In order to model a deep excavation that is dry, pore water pressure imbalance at the retaining wall must be created manually by using pressure boundary condition at the soil-structure interface of the retaining wall as shown in Figure 3(b).

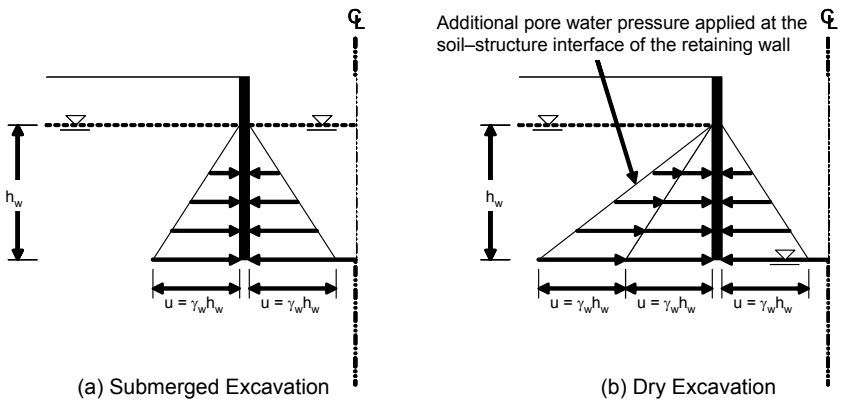

(a) Submerged Excavation (b) Dry Excavation

Fig. 3 Simulation of Submerged and Dry Excavations in PLAXIS

Simulation of Construction Details

A detailed description of various construction stages for the Chicago Subway Renovation Project can be found in Calvello (2002), Finno et al. (2002) and Calvello and Finno (2004). For the purpose of back analysis, eight construction stages have been identified. Schematic drawings of these eight stages are shown in Figure 4. The details of construction activity for each stage are given in Table 1.

Simulation of tunnel construction (Stage 1) is achieved by removing the soil elements occupying the tunnel cross-sectional area and adding structural elements that represent the lining of the tunnel. There will inevitably be ground deformations in response to tunnel construction; however, at the end of Stage 1, such ground deformations are reset to zero but the stress changes are retained. In this way, it is possible to achieve a realistic stress distribution within the soil prior to the installation of the retaining wall and its support system.

Table 1 Details of various stages of construction for Chicago Subway Renovation Project

Stage	*Activity*	*Description*	*Ground Condition*
1	Tunnel construction	(a) Simulate tunnel construction.	Undrained plastic
		(b) Allow consolidation. Reset ground deformations resulting from tunnel construction to zero.	Consolidation
2	Wall installation	(a) Simulate installation of secant pile wall as wished-in-place.	Undrained plastic
		(b) Allow consolidation. Reset ground deformation resulting from wall installation to zero.	Consolidation
3	Excavation and installation of props and anchors	Excavate first layer of soil [4.5 m]. Install horizontal prop.	Undrained plastic
4		Excavate second layer of soil [1.0 m].	Undrained plastic
5		Install first anchor rod and pre-stress it to 220 kN/m.	Undrained plastic
6		Excavate third layer of soil [4.0 m].	Undrained plastic
7		Install second anchor rod and pre-stress it to 290 kN/m.	Undrained plastic
8		Excavate the final layer of soil [2.5 m]	Undrained plastic

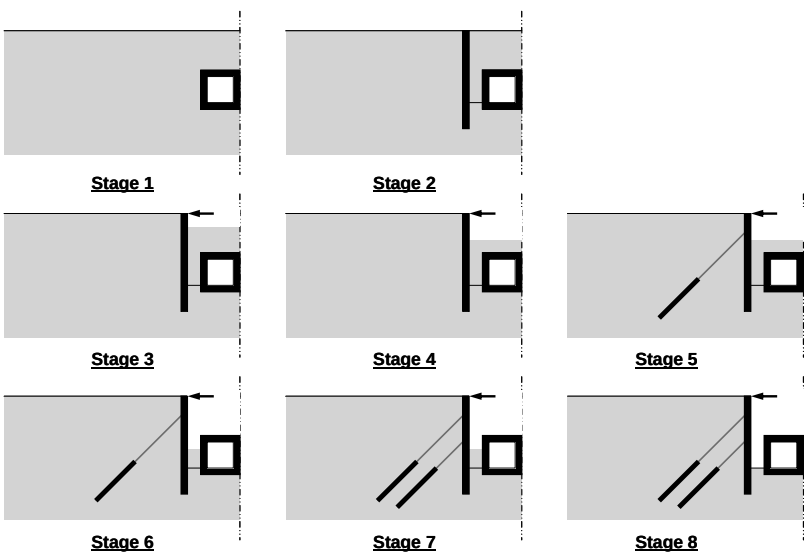

Fig. 4 Schematic Diagrams of Various Stages of Construction for Chicago Subway Renovation Project

Simulation of installation of the secant pile retaining wall (Stage 2) is achieved in a manner similar to the installation of the tunnel lining, i.e. the structural elements representing the retaining wall are simply added to the finite element mesh, thereby achieving what is known as 'wished-in-place' (WIP) modelling of retaining wall installation (De Moor 1994). WIP modelling does not take into account the unloading and subsequent deformation of the ground adjacent to the retaining wall. Such unloading and deformation of the ground during retaining wall installation can be modelled using a 'wall-installation-modelled' (WIM) analysis (De Moor 1994); however, it is not a trivial task to conduct a WIM analysis using PLAXIS. It can be argued that the focus of the research is not the simulation of retaining wall installation but the effect of deep excavation on adjacent ground, and for this purpose, a WIP modelling of retaining wall installation is deemed sufficient.

Excavation of soil layers (Stages 3, 4, 6, and 8) is achieved by removing the elements representing these soil layers. The stress change resulting from the removal of soil layers is subdivided into several small increments of stress change using the automatic load stepping option available in PLAXIS.

Installation of anchor (tie back) rods (Stages 5 and 7) is achieved by activating the structural elements representing the anchor rods. The grouted portion of an anchor rod is connected with adjacent finite element nodes using interface elements, and the remaining portion of the anchor rod is connected to the finite element mesh only at the end nodes. The pre-stressing option available in PLAXIS is used to apply a pre-stressing load on an anchor rod.

Details of the Back Analyses

Several different types of back analyses of the Chicago Subway Renovation Project deep excavation were conducted using PLAXIS. The details of these back analyses in terms of the different constitutive models used for various soil layers and their input parameters are provided in this Section. Table 2 gives brief descriptions of these back analyses.

For analyses CAL-D and CAL-S, the finite element mesh is shown in Figure 5 and the constitutive models used for the various soil layers and their input parameters are given in Table 3. The input parameters for the structural elements used in analyses CAL-D and CAL-S are given in Table 4. For analyses SIM-O and SIM-M, the finite element mesh is shown in Figure 6 and the constitutive models used for various soil layers and their input parameters are given in Table 5. The input parameters for the structural elements used in analyses SIM-O and SIM-M were exactly the same as those used for analyses CAL-D and CAL-S (Table 4). The finite element meshes and model input parameters for analyses SIM-NT and SIM-C were the same as those for analysis SIM-M except that there was no tunnel present inside the deep excavation in the finite element mesh for analysis SIM-NT.

Table 2 Brief Descriptions of the Back-Analyses of Chicago Subway Renovation Project

Analysis Identifier	Analysis Description
CAL-D	Repetition of back analysis done by Calvello (2002); simulation of dry deep excavation; no simplification of stratigraphy; input parameters same as those used by Calvello (2002).
CAL-S	Same as CAL-D except for simulation of submerged deep excavation.
SIM-O	Simplification of stratigraphy by combining the clay crust, Upper Blodgett, Lower Blodgett, Deerfield and Park Ridge layers into one "soft glacial clay" layer with undrained shear strength linearly increasing with depth; simulation of dry deep excavation; stiffness parameters for the soft glacial clay layer obtained by matching the horizontal displacement of the retaining wall and the vertical settlement of the backfill with those computed using CAL-D.
SIM-M	Same as SIM-O except stiffness parameters for the soft clay layer adjusted by matching the horizontal displacement of the retaining wall and the vertical settlement of the backfill with those observed in the field.
SIM-NT	Same as SIM-M except there is no tunnel present inside the deep excavation.
SIM-C	Same as SIM-M except incorporation of waiting period between two successive excavation sequences.

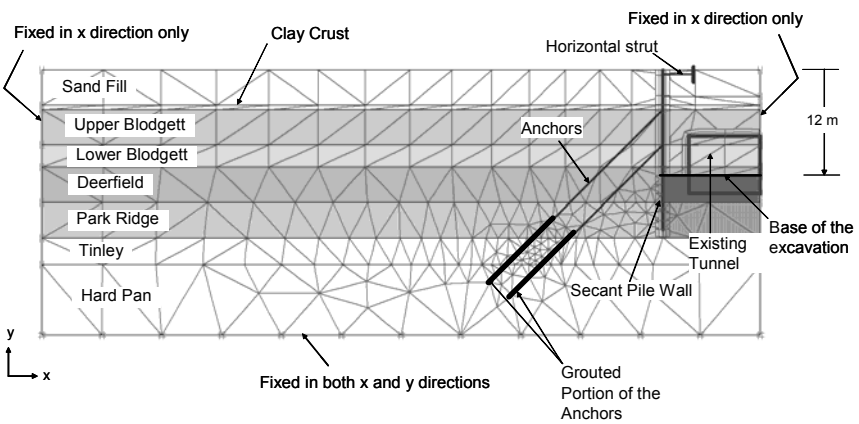

Fig. 5 Finite Element Mesh Used in Analyses CAL-D and CAL-S

Table 3 Input Parameters for Various Soil Layers for Analyses CAL-D and CAL-S

Soil Type:	Sand Fill	Clay Layers						Hard Pan
		Clay Crust	Upper Blodgett	Lower Blodgett	Deer-field	Park Ridge	Tinley	
Model:	MC	HS	HS	HS	HS	HS	HS	MC
Behaviour: Parameter (Symbol, Unit)	D	U	U	U	U	U	U	U
Unit weight above water table (Γ_{unsat},kN/m^3)	17.0	17.7	16.1	16.1	16.9	17.6	17.6	18.4
Unit weight below water table (Γ_{sat}, kN/m^3)	19.0	19.7	18.1	18.1	18.9	19.6	19.6	20.4
Horiz. Permeability (K_x, cm/day)	150	0.015	0.015	0.015	0.015	0.015	0.015	0.015
Vertical permeability (K_y, cm/day)	150	0.0092	0.0092	0.0092	0.0092	0.0092	0.0092	0.0092
Secant modulus (E_{50}^{ref}, kPa)	-	40500	4700	6000	6000	8000	12900	-
Oedometer modulus (E_{oed}^{ref}, kPa)	-	28350	3290	4200	4200	6020	9030	-
Unload-reload modulus (E_{ur}^{ref}, kPa)	-	121500	14100	18000	18000	25800	38700	-
Power for stress law (m)	-	0.80	0.80	0.80	0.85	0.85	0.85	-
Poisson's ratio (μ)	0.33	0.20	0.35	0.35	0.35	0.35	0.20	0.20
Earth pressure coefficient (K_0)	0.43	0.47	0.60	0.60	0.57	0.46	0.46	0.43
Cohesion intercept (c, kPa)	2.0	1.0	1.0	1.0	1.0	1.0	1.0	100.0

Table 3 Contd. Input Parameters for Various Soil Layers for Analyses CAL-D and CAL-S

Soil Type:	Sand Fill	Clay Layers						Hard Pan
		Clay Crust	Upper Blodgett	Lower Blodgett	Deer-field		Park Ridge	Tinley
Friction angle (ϕ, °)	35.0	32.0	23.4	23.4	25.6	25.6	32.8	35.0
Dilatancy angle (ψ, °)	5.0	0.0	0.0	0.0	0.0	0.0	0.0	3.0
Young's Modulus at the top of a layer (E_0, kPa)	18000	-	-	-	-	-	-	147000
Rate of increase of Young's Modulus with depth (m_E, kPa/m)	0.0	-	-	-	-	-	-	0.0
Strength Reduction Factor (R_f)	-	0.9	0.9	0.9	0.9	0.9	0.9	-
Interface strength ratio (R_{int})	0.8	0.5	1.0	1.0	1.0	0.5	0.5	0.5

[Note: MC – Mohr-Coulomb Model; HS – Hardening Soil Model; D – Drained; U – Undrained.]

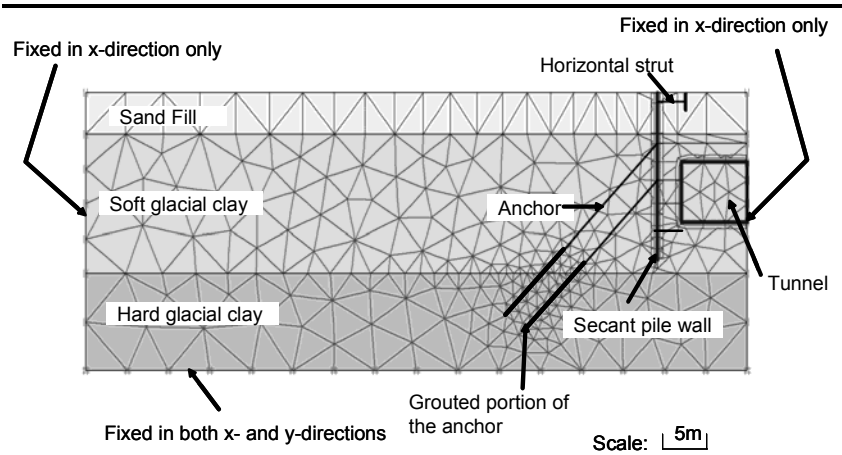

Fig. 6 Finite Element Mesh Used in Analyses SIM-O and SIM-M

Table 4 Input Parameters for Various Structural Elements for Analyses CAL-D and CAL-S

Element:			Tunnel Lining	Secant Pile Wall	Grouted Anchor
Model:			Plate	Plate	Anchor
Behaviour:			Elastic	Elastic	Elastic
Parameter	Symbol	Units			
Normal stiffness	*EA*	kN/m	1.40E+07	6.50E+06	2.60E+05
Flexural rigidity	*EI*	kNm^2/m	1.43E+05	1.00E+05	-
Equivalent thickness	*d*	m	0.35	0.43	-
Weight	*w*	kN/m	8.4	10.3	-
Poisson's ratio	μ	-	0.15	0.2	-
Anchor spacing	L_s	m	-	-	1.5
Pre-stress force	-	kN/m	-	-	-
Element:			Horizontal Strut	Top Anchor	Bottom Anchor
Model:			Fixed Anchor	Anchor	Anchor
Behaviour:			Elastic	Elastic	Elastic
Parameter	*Symbol*	Units			
Normal stiffness	*EA*	kN/m	6.75E+05	1.84E+05	2.30E+05
Flexural rigidity	*EI*	kNm2/m	-	-	-
Equivalent thickness	*d*	m	-	-	-
Weight	*w*	kN/m	-	-	-
Poisson's ratio	□	-	-	-	-
Anchor spacing	*Ls*	m	6	1.5	1.5
Pre-stress force	-	kN/m	-	220	290

[Note: *E* – Young's modulus, *A* – cross-sectional area; *I* – moment of inertia.]

Table 5 Soil Input Parameters for Analyses SIM-O and SIM-M

Soil Type:			Sand Fill	Soft Glacial Clay	Hard Glacial Clay
Model:			Mohr-Coulomb	Hardening Soil	Mohr-Coulomb
Behaviour:			Drained	Undrained	Undrained
Parameter		Units			
Unit weight above water table	γ_{unsat}	kN/m^3	17.0	16.4	18.0
Unit weight below water table	γ_{sat}	kN/m^3	19.0	18.4	20.0
Horizontal permeability	K_x	cm/day	150	0.01	0.01
Vertical permeability	K_y	cm/day	150	0.01	0.01
Secant modulus	E_{50}^{ref}	kPa	-	2900	-
Oedometer modulus	E_{oed}^{ref}	kPa	-	2900	-
Unload-reload modulus	E_{ur}^{ref}	kPa	-	8700	-
Power for stress law	m	-	-	1.0	-
Reference mean stress	p^{ref}	kPa	-	100	-
Poisson's ratio	μ	-	0.33	0.35*	0.33
Earth pressure coefficient	K_o	-	0.52	0.52	0.52
Cohesion intercept	c	kPa	2.0	-	130.0
Friction angle	ϕ	°	35.0	-	35.0
Dilatancy angle	ψ	°	5.0	-	5.0
Undrained Shear Strength at the top of the layer	S_{UO}	kPa	-	20	-
Young's Modulus at the top of the layer	E_O	kPa	18000	-	65000
Strength reduction factor	R_f	-	-	0.7	-
Interface strength ratio	R_{int}	-	0.8	0.8	0.8
Rate of increase of undrained shear strength with depth	m_C	kPa/m	-	7.33	-
Rate of increase of Young's Modulus with depth	m_E	kPa/m	0	-	500

[Note: *Effective Poisson's ratio; PLAXIS automatically selects a value of 0.495 if undrained option is specified.]

Results

Analysis CAL-D

Figure 7 shows the comparison between the observed horizontal displacement of the retaining wall due to deep excavation and the horizontal displacement of the retaining wall computed by analysis CAL-D. Figure 8 shows a comparison between the observed ground settlement (east side of the excavation; underneath the raft foundation of the school) behind the retaining wall and the ground settlement computed by analysis CAL-D. It is clear that analysis CAL-D, which simulated a dry deep excavation, overestimated both the horizontal displacement of the retaining wall and the ground settlement behind the retaining wall considerably. This observation is not consistent with that reported by Calvello (2002), whose analysis provided reasonably close predictions of both horizontal displacement of the retaining wall and the ground settlement behind the retaining wall.

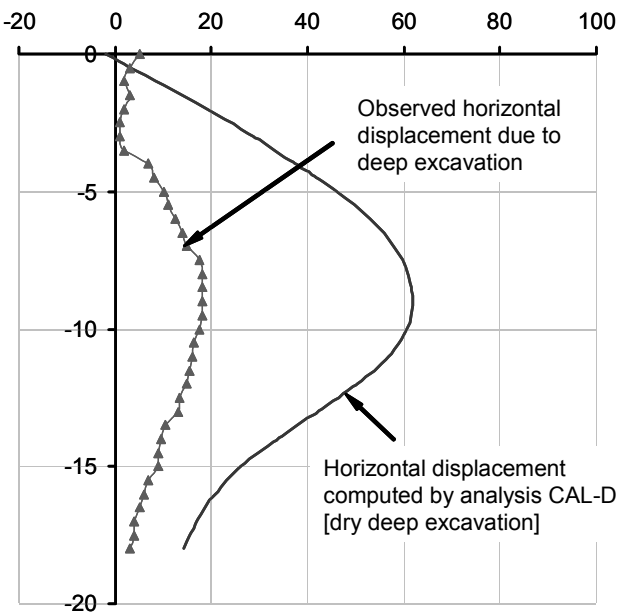

Fig. 7 Observed and Computed Horizontal Displacement of the Retaining Wall – Analysis CAL-D

Although it is fairly obvious that the deep excavation must have been kept dry during construction for the purpose of installing tie-back anchors, it could not be established whether a dry deep excavation was actually modelled by Calvello (2002). As explained above, the default option in PLAXIS is to treat a deep excavation as submerged. Perhaps, Calvello (2002) obtained good matching between the observed and computed results because of choosing this default option. It was, therefore, decided to conduct analysis CAL-S in which the same deep excavation was modelled as submerged.

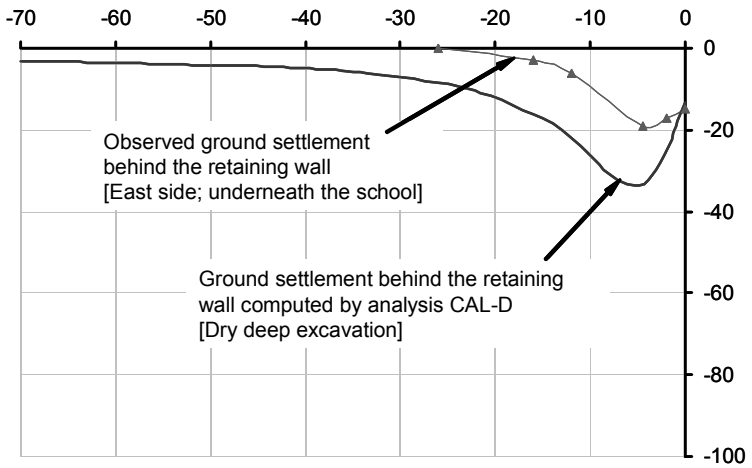

Fig. 8 Observed and Computed Ground Settlement Behind the Retaining Wall – Analysis CAL-D

Analysis CAL-S

Analysis CAL-S was exactly the same as analysis CAL-D except that the deep excavation was modelled as submerged, i.e. there was no imbalance of pore-water pressure between the inside and the outside of the retaining wall.

Figure 9 shows a comparison between the observed horizontal displacement of the retaining wall due to deep excavation and the horizontal displacement of the retaining wall computed by analysis CAL-S. Figure 10 shows a comparison between the observed ground settlement (east side of the excavation; underneath the raft foundation of the school) behind the retaining wall and the ground settlement computed by analysis CAL-S. It can be seen that the agreement between the observed and the computed horizontal displacement of the retaining wall is fairly close.

The values of computed ground settlement behind the retaining wall, however, are less than the observed ground settlement values. One possible reason for this discrepancy could be the fact that the observed ground settlement values were from the east side of the excavation, underneath the raft foundation for the school, and that the presence of school was not incorporated in any of the back analyses reported herein. The bearing pressure of the raft foundation for the school could have resulted in a higher ground settlement behind the retaining wall.

The reasonably close agreement obtained between the observed and computed values of horizontal displacement and ground settlements by modelling the deep excavation as submerged, suggests that Calvello (2002) probably modelled the deep excavation as submerged instead of modelling it as dry. It also highlights potential pitfalls of using a finite element back analysis to calibrate soil parameters and the importance of accurate modelling of construction processes for such calibration.

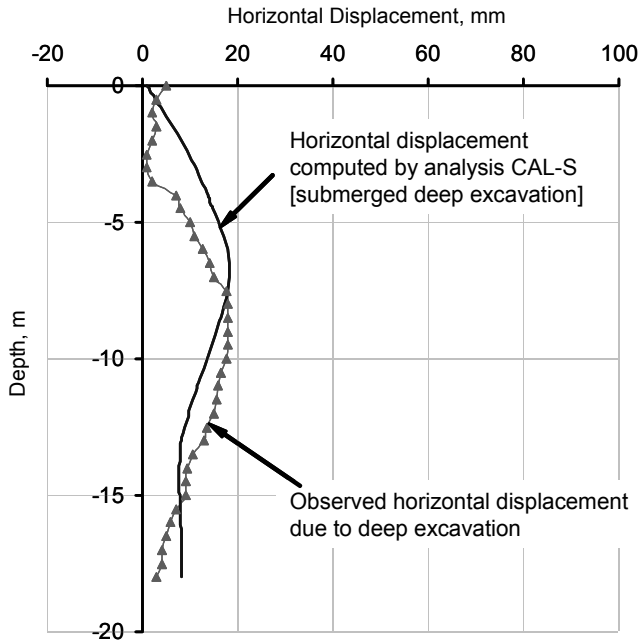

Fig. 9 Observed and Computed Horizontal Displacement of the Retaining Wall – Analysis CAL-S

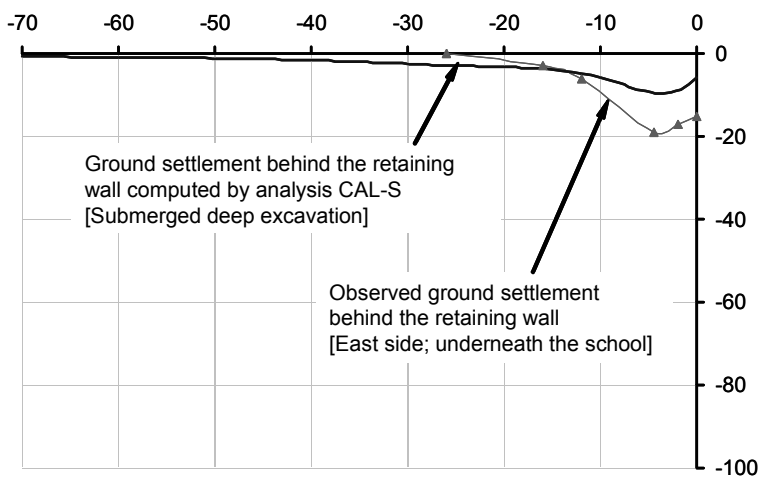

Fig. 10 Observed and Computed Ground Settlement Behind the Retaining Wall – Analysis CAL-S

Analysis SIM-O

Incorporation of a reasonably accurate soil stratigraphy is important in a finite element back analysis of deep excavation. However, the greater the number of layers, the more difficult it is to quantify the effect of a parameter, e.g. soil stiffness or soil undrained shear strength, on the overall behaviour of the structure. It was, therefore, decided to simplify the soil stratigraphy for the Chicago Subway Renovation Project by combining the five glaciated clay layers, i.e. clay crust, Upper Blodgett, Lower Blodgett, Deerfield and Park Ridge, into a single layer termed “soft glacial clay”, and combining the Tinley and Hard Pan layers into another single layer termed “hard glacial clay”. Analysis SIM-O was done using this simplified soil stratigraphy.

The soft glacial clay layer and the hard glacial clay layer were modelled using the Hardening Soil model and the Mohr-Coulomb model, respectively. The behaviour of the soft glacial clay layer was modelled as undrained and its undrained shear strength was assumed to increase linearly with depth at a rate of 7.33 kPa/m. Such a straight line variation of undrained shear strength with depth was obtained by fitting a straight line through the undrained shear strength values of the five component strata obtained by Roboski (2001) using vane shear testing, pocket penetrometer, unconfined compression tests and triaxial compression/extension tests, as shown in Figure 11. The undrained shear strength at the top of the soft glacial clay layer was taken equal to 20 kPa.

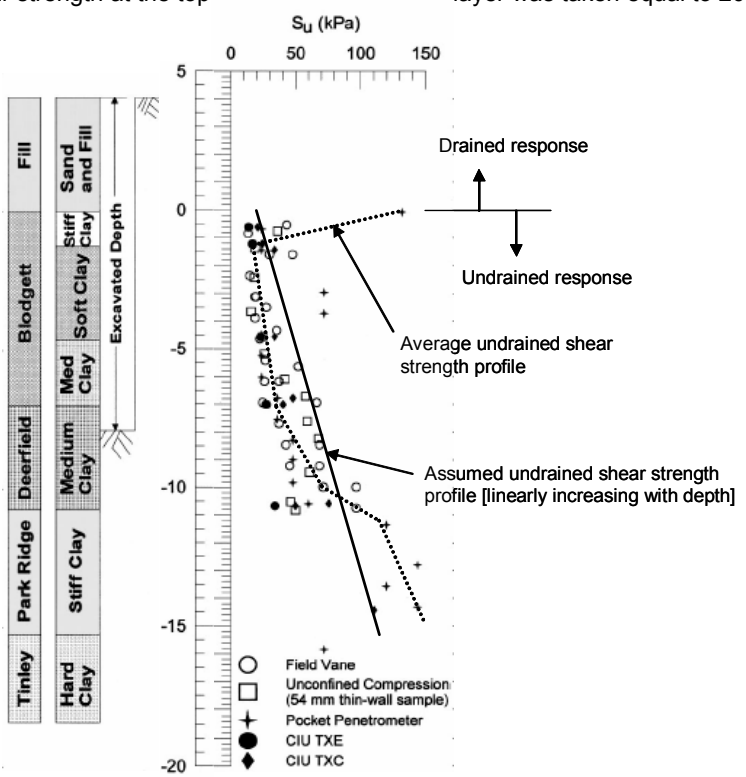

Fig. 11 Undrained Shear Strength Profile Used in Analysis SIM-O (Based on Data Given in Roboski 2001)

The sequence of construction modelled in analysis SIM-O was exactly the same as that used for analysis CAL-D (see Figure 4 and Table 1). For the hard glacial clay layer, the soil parameters were obtained by taking the average of soil parameters for the Tinley and Hard Pan strata. For the soft glacial clay, the soil parameters (with the exception of undrained shear strength) were obtained using a calibration procedure in which the horizontal displacement of the retaining wall computed using analysis SIM-O was matched with that computed by analysis CAL-D. The matching was achieved by adjusting only the reference secant stiffness, E_{50}^{ref}, for the soft glacial layer (shown in **bold** typeface in Table 5). The reference oedometer stiffness, E_{oed}^{ref}, was taken equal to the reference secant stiffness and the reference unload-reload stiffness, E_{ur}^{ref}, was taken equal to three times the reference secant stiffness. Theoretically, soil stiffness parameters for each of the three layers must be calibrated using the matching procedure described above; however, the overall behaviour of the retaining wall and the surrounding ground would be dominated by the soft glacial clay layer because (a) this layer has the least stiffness and strength; and, (b) the deep excavation is located almost entirely within this layer.

Figure 12 shows the distributions of horizontal displacement of the retaining wall with depth computed by analysis SIM-O (E_{50}^{ref} = 2900 kPa) and analysis CAL-D.

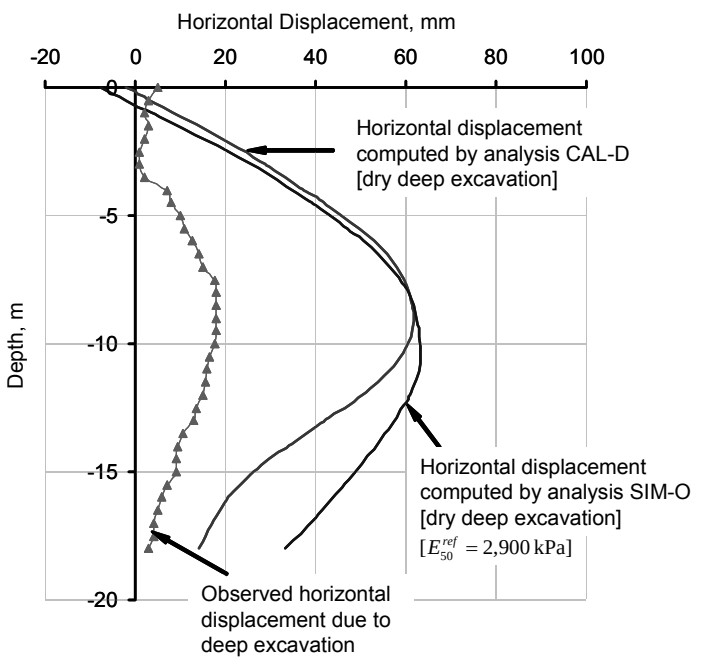

Fig. 12 Matched Horizontal Displacement of the Retaining Wall – Analyses SIM-O and CAL-D

The match is quite good up to 9 m depth. Beyond 9 m depth, the horizontal displacements computed by analysis SIM-O are more than those computed by analysis CAL-D. Poor matching beyond 9 m depth can be attributed to the fact that the stiffness of the soft glacial clay layer used in analysis SIM-O is less than the stiffness of Deerfield and Park Ridge strata used in analysis CAL-D. Given that the deep excavation is only 12 m deep, it is encouraging to see good matching of horizontal displacements computed by analyses SIM-O and CAL-D for most of the depth of excavation.

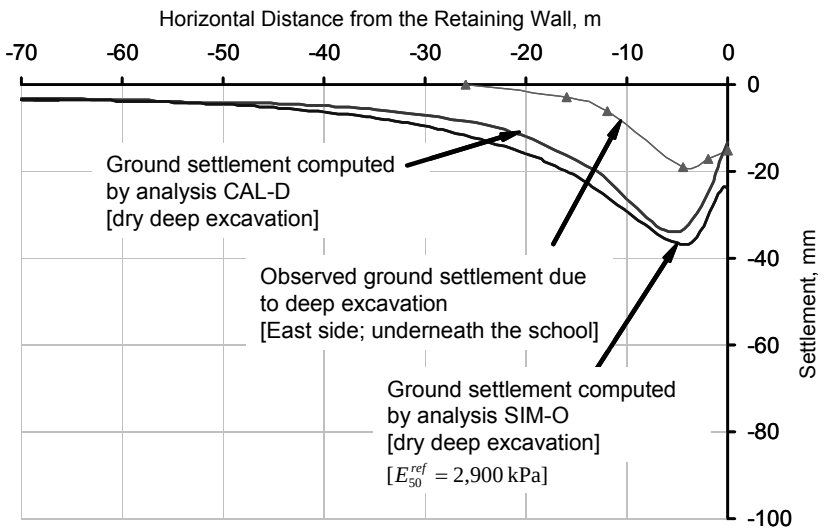

Fig. 13 Matched Ground Settlement Behind the Retaining Wall – Analyses SIM-O and CAL-D

Figure 13 shows the distributions of ground settlement behind the retaining wall computed by analyses SIM-O and CAL-D. It can be seen that the matching is reasonably good for a horizontal distance of up to 70 m from the retaining wall even though matching of ground settlement was not sought in the calibration procedure described above. Good matching of both the horizontal displacement of the retaining wall and the ground settlement behind the retaining wall between analyses SIM-O and CAL-D suggests that analysis SIM-O, which was conducted using a simplified stratigraphy, was able to capture the pattern of ground deformation around the deep excavation satisfactorily. It should now be possible to increase the E_{50}^{ref} value of the soft glacial clay layer to match the observed horizontal displacement of the retaining wall; this is done using analysis SIM-M described in the next section.

Analysis SIM-M

Analysis SIM-M was exactly the same as analysis SIM-O except for the value of reference secant stiffness, E_{50}^{ref}, for soft glacial clay, which was increased in steps until the computed values of horizontal displacement of the

retaining wall matched reasonably well with the observed values. A reasonably good match between computed and observed horizontal displacement values was obtained for E_{50}^{ref} = 17000 kPa as shown in Figure 14.

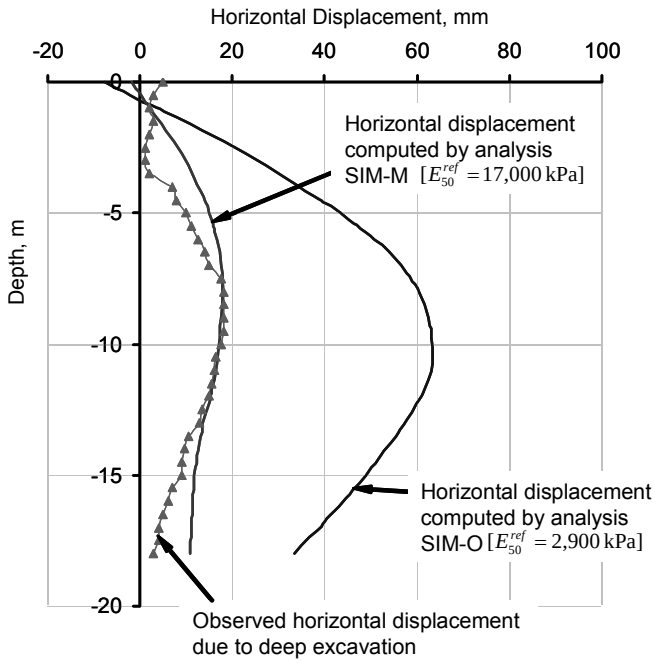

Fig. 14 Horizontal Displacement of the Retaining Wall Computed by Analyses SIM-O and SIM-M

The matching of computed and observed ground settlement behind the retaining wall (Figure 15), however, was not as good as the matching of horizontal displacement. As explained above, the observed ground settlement profile was obtained from the east side of the deep excavation underneath the raft foundation of the school, and therefore, it was probably affected by the bearing pressure of the raft foundation. In other words, ground settlements on the west side of the excavation, which were not monitored, would have been considerably less than those observed underneath the raft foundation of the school and would have plotted reasonably close to those computed by analysis SIM-M. It can, therefore, be concluded that both the pattern and the magnitude of ground deformation around the deep excavation can be controlled reasonably accurately using the stiffness of soft glacial clay.

Analysis SIM-NT

The deep excavation for Chicago Subway Renovation Project is unusual because of the presence of a tunnel inside the deep excavation. It is important to quantify the effect of the presence of this tunnel inside the deep excavation; therefore, analysis SIM-NT, which had no tunnel inside the deep excavation, was conducted. The results obtained from analysis SIM-NT were compared with

those obtained from analysis SIM-M, which had tunnel inside the deep excavation.

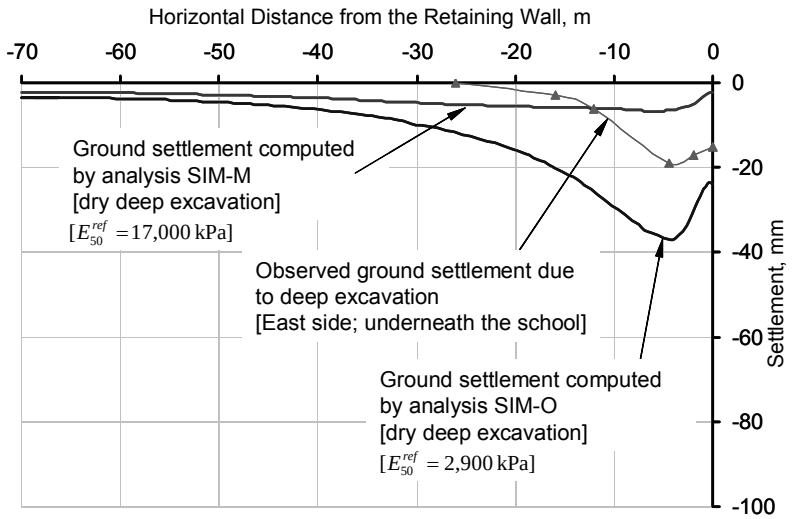

Fig. 15 Ground Settlement Behind the Retaining Wall Computed by Analyses SIM-O and SIM-M

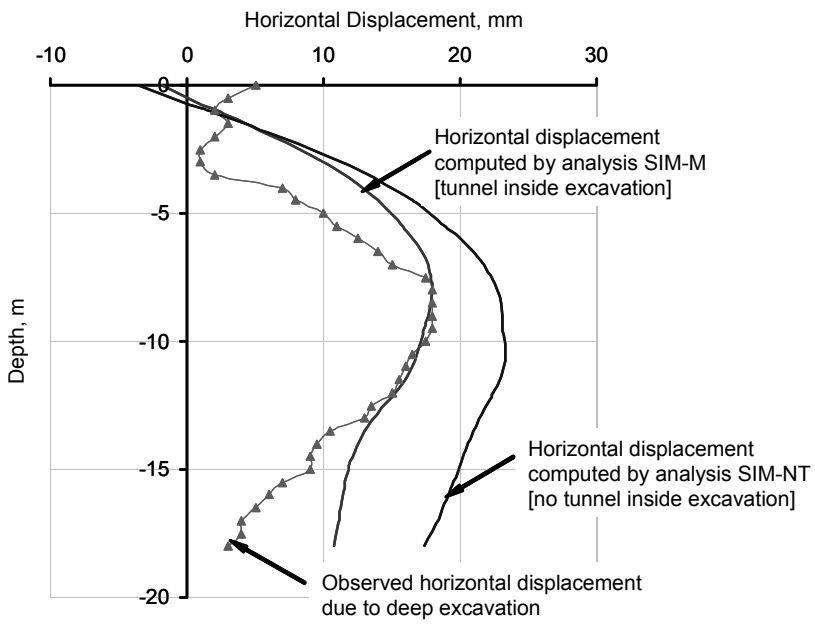

Fig. 16 Horizontal Displacement of the Retaining Wall Computed by Analyses SIM-NT and SIM-M

Figure 16 shows the distribution of horizontal displacement of the retaining wall with depth computed by analyses SIM-NT and SIM-M. It is evident from Figure 16 that the tunnel provides some lateral support to the retaining wall, thereby reducing its horizontal displacement.

Analysis SIM-C

For a deep excavation having dimensions comparable to the dimensions of the deep excavation for Chicago Subway Renovation Project, there is usually a waiting period between two successive excavations of soil layers. During this waiting period, several important activities take place, such as dewatering of the excavation, installation of struts, braces and anchors, etc. If the permeability of the ground is sufficiently high, excess pore-water pressures induced by the excavation could potentially dissipate, resulting in consolidation (and deformation) of the surrounding ground. On the other hand, if the ground is fairly impermeable (i.e., having hydraulic conductivity less than 10^{-7} m/s), there would be very little change in pore-water pressure during the waiting period and the behaviour of the ground can be modelled as undrained.

There were several waiting periods for the Chicago Subway Renovation Project deep excavation (Finno et al. 2002). It was, therefore, decided to conduct analysis SIM-C, which modelled consolidation of the surrounding ground during waiting periods between successive excavation sequences. The results of analysis SIM-C were then compared with the results of analysis SIM-M in which there was no waiting period between successive excavation sequences.

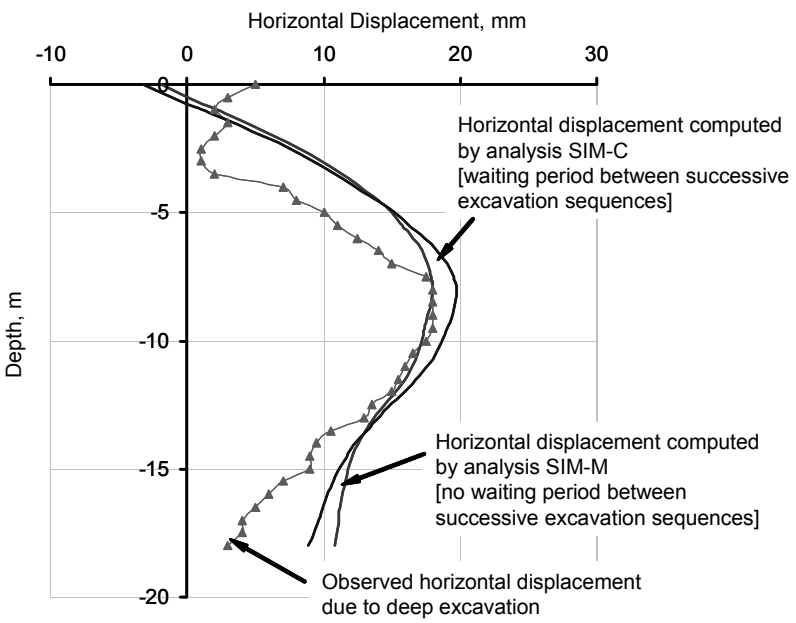

Fig. 17 Horizontal Displacement of the Retaining Wall Computed by Analyses SIM-C and SIM-M

Figure 17 shows the distribution of horizontal displacement of the retaining wall computed by analyses SIM-C and SIM-M. It can be seen from Figure 17 that there is a slight increase in the maximum horizontal displacement of the retaining wall above the base of the excavation and a slight decrease in the horizontal displacement of the retaining wall below the base of the excavation when consolidation during waiting periods is modelled. The increase in the maximum horizontal displacement of the wall above the base of the excavation is likely due to consolidation settlement of the ground behind the retaining wall. One possible reason for the decrease in the horizontal displacement of the retaining wall below the base of the excavation could be the stiffening of the ground underneath the tunnel caused by dissipation of excess pore-water pressures during the waiting periods. For all practical purposes, however, the effect of modelling consolidation of the surrounding ground during waiting periods is not significant, and therefore, analysis SIM-M, which does not incorporate waiting periods between successive excavation sequences, can be considered to model the overall behaviour of the deep excavation adequately.

Parametric Study

In this Section, the details and the results of a parametric study based on the Chicago Subway Renovation Project deep excavation are presented. The following parameters were varied: reference secant stiffness of the soft glacial clay layer [E_{50}^{ref}]; and, the stiffness of the secant pile wall represented by its thickness [t_R]. When one of these two parameters was varied, the other parameter was held constant. The effect of varying a parameter was quantified by obtaining the variation in the following three quantities: δh_{max} - maximum horizontal displacement of the retaining wall; δv_{max} - maximum ground settlement behind the retaining wall; and, BM_{max} - maximum bending moment in the retaining wall. For all the analyses conducted for the purpose of this parametric study, the following quantities or features were unchanged:

- Rate of increase of undrained shear strength with depth (m_C = 7.33 kPa/m);
- All the parameters for the other two soil layers, i.e. sand fill and hard glacial clay;
- Parameters and locations of all the structural components such as tunnel lining, horizontal strut, anchors, etc;
- Depth of the excavation (H =12 m), the construction sequences, and the finite element mesh.

Since analysis SIM-M, which incorporated a simplified stratigraphy, was able to reproduce both the pattern and the magnitude of ground deformation for the deep excavation, it was used as the base case for the parametric study. The values of the two parameters for the base case were: $[E_{50}^{ref}]_{BC}$ = 16000 kPa; and, $[t_R]_{BC}$ = 1.0 m. The results of the parametric study are presented as normalized changes in parameters and quantities as shown in Table 6. The ranges for the two parameters are given in Table 7 (base case values highlighted in **bold** face).

Table 6 Normalized Changes in Parameters and Quantities for the Parametric Study

Parameter or quantity	Symbol	Formula
Normalized change in reference secant stiffness	ΔE_N	$\Delta E_N = \frac{E_{50}^{ref} - \left[E_{50}^{ref}\right]_{BC}}{\left[E_{50}^{ref}\right]_{BC}}$
Normalized change in thickness of the secant pile retaining wall	Δt_N	$\Delta t_N = \frac{t_R - \left[t_R\right]_{BC}}{\left[t_R\right]_{BC}}$
Normalized change in maximum horizontal displacement of the retaining wall	Δh_N	$\Delta h_N = \frac{\delta h_{max} - \left[\delta h_{max}\right]_{BC}}{\left[\delta h_{max}\right]_{BC}}$
Normalized change in maximum ground settlement behind the retaining wall	Δv_N	$\Delta v_N = \frac{\delta v_{max} - \left[\delta v_{max}\right]_{BC}}{\left[\delta v_{max}\right]_{BC}}$
Normalized change in maximum bending moment in the retaining wall	ΔBM_N	$\Delta BM_N = \frac{BM_{max} - \left[BM_{max}\right]_{BC}}{\left[BM_{max}\right]_{BC}}$

Table 7 Range of Values of Parameters for the Parametric Study

Parameter	Units	Range of Values used in the Parametric Study								
E_{50}^{ref}	kPa	4000	8000	12000	**16000**	20000	24000	28000	32000	48000
ΔE_N	-	-0.75	-0.5	-0.25	**0.00**	0.25	0.50	0.75	1.00	2.00
t_R	m	0.4	0.6	0.8	**1.0**	1.2	1.4	1.6		
Δt_N	-	-0.6	-0.4	-0.2	**0.0**	0.2	0.4	0.6		

[Note: The parameters for the base case are shown in **bold**.]

Effect of Soil Stiffness

Figure 18 shows the effect of change in soil stiffness on the maximum horizontal displacement of the retaining wall, maximum ground settlement behind the retaining wall and the maximum bending moment induced in the retaining wall due to deep excavation. A significant increase in the ground deformation around the deep excavation is observed when the soil stiffness is decreased from its value for the base case. The maximum bending moment in the retaining wall also increases in response to decrease in soil stiffness; however, the increase in maximum bending moment is less than the increase in horizontal displacement or ground settlement. Similarly, a decrease in ground deformation and a decrease in bending moment in the retaining wall are observed when the soil stiffness is increased from its value for the base case; however, the effect of increasing the soil stiffness is much less compared with the effect of decreasing the soil stiffness.

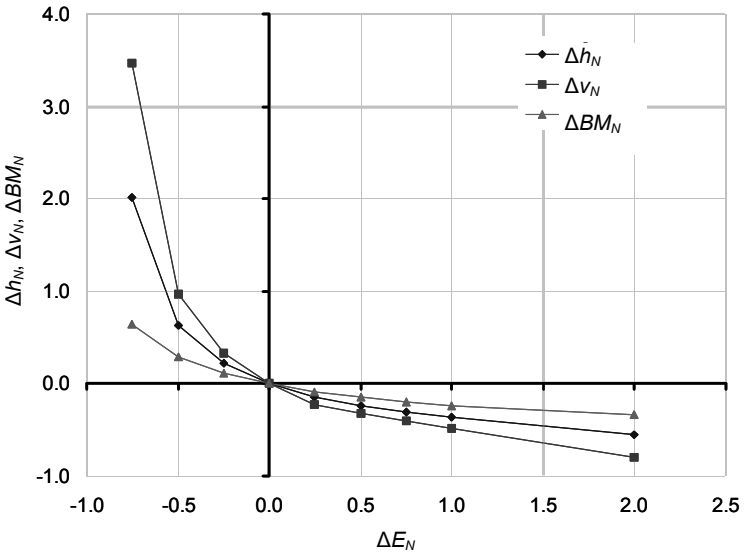

Fig. 18 Effect of Change in Soil Stiffness on Horizontal Displacement of the Retaining Wall, Ground Settlement Behind the Retaining Wall and Bending Moment in the Retaining Wall

Effect of Stiffness of the Retaining Wall

Since the Young's modulus of the retaining wall was kept unchanged for all the analyses, a change in thickness of the retaining wall represents a change in both the bending stiffness and the axial stiffness of the retaining wall. Figure 19 shows the effect of change in thickness of the retaining wall on the maximum horizontal displacement of the retaining wall, maximum ground settlement behind the retaining wall and the maximum bending moment induced in the retaining wall due to deep excavation.

It can be seen from Figure 19 that the effect of change in thickness of the retaining wall is not as prominent as the change in soil stiffness; however, it is more significant than the effect of change in soil undrained shear strength. It is interesting to note that the maximum bending moment in the retaining wall increases but the horizontal displacement of the retaining wall decreases when the thickness of the retaining wall is increased. Clearly, a thicker retaining wall is able to resist horizontal deformation better but at the expense of inducing greater bending moment. In other words, a stiffer retaining wall also needs greater bending strength. It is also worth noting that the horizontal displacement of the retaining wall does not reduce appreciably but the maximum bending moment continues to increase when the thickness of the retaining wall is increased by more than 40%. This implies that it is not useful to increase the stiffness of the retaining wall beyond a certain maximum value.

The horizontal displacement of the retaining wall and the ground settlement behind the retaining wall show contrasting trends with the change in thickness of the retaining wall. The horizontal displacement of the retaining wall decreases but the ground settlement behind the retaining wall increases as the thickness of the retaining wall is increased. In the case of a stiffer retaining wall,

the ground is prevented from spreading horizontally. The deformation of the ground, therefore, occurs mainly in the vertical direction, resulting in an increase in ground settlement behind the retaining wall. In other words, consolidation of the ground behind a stiff retaining wall is mainly one-dimensional. For a relatively flexible retaining wall (smaller thickness), there is a reduction in horizontal stresses in the ground behind the retaining wall, which results in increase in horizontal displacement.

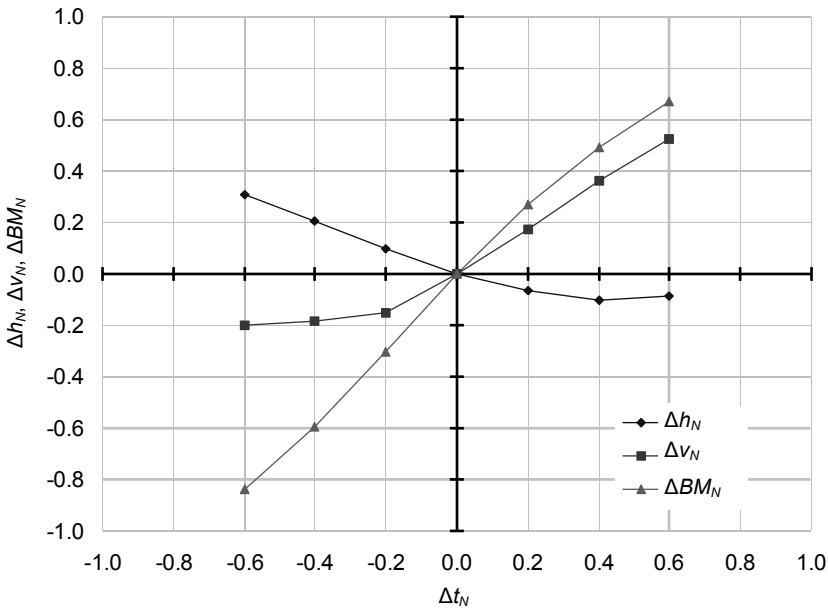

Fig. 19 Effect of Change in Thickness of the Retaining Wall on Horizontal Displacement of the Retaining Wall, Ground Settlement Behind the Retaining Wall and Bending Moment in the Retaining Wall

Conclusions

The mechanisms of soil-structure interaction in and around a braced deep excavation were investigated using finite element back-analysis of an instrumented case study as well as using a parametric study. Based on the results of the finite element back-analysis, it can be concluded that it is important to model the construction processes accurately when using back-analysis (or inverse analysis) to calibrate soil parameters. The modeller must be aware of specific procedures prescribed by the modelling software to model these construction sequences. It is demonstrated that it is possible to capture both the pattern and the magnitude of ground deformation around a deep excavation using a simplified stratigraphy obtained by grouping several successive soil layers into one layer; however, there must be some physical basis for such grouping and the combined layer must represent (or dominate) the overall behaviour of the ground. The physical basis could be the common origin of these soil layers or common type of soil behaviour. In case of Chicago

Subway Renovation Project, the grouping was done on the basis of the observation that all the grouped layers were clays of glacial origin which exhibited undrained shear strength linearly increasing with depth. This result also confirms the classical modelling paradigm of keeping the model simple enough but not any simpler.

From the results of the parametric study, it can be concluded that the stiffness of the soil and the stiffness of the retaining wall influence the deformation of the ground surrounding the deep excavation significantly. It is important to obtain accurate estimates of soil stiffness in order to obtain accurate estimates of ground deformation. It is also important to appreciate that even the stiffest of retaining walls will result in some horizontal displacement of the ground. If the major concern is to limit the ground settlement behind the retaining wall during a deep excavation, it might be better to use a slightly flexible retaining wall system for temporary support of the excavation. A flexible retaining wall appears to induce lower ground settlements in the short-term, i.e. during the excavation. Long-term effects of using a flexible retaining wall as permanent support for a deep excavation were not investigated in the present study.

References

Athanasiu, C.M., Simonsen, A.S. and Ronning, S. (1991): 'Back-calculation of case records to calibrate soil-structure interaction analysis by finite element method of deep excavation in soft soil', *Proc. 10th European Conference on Soil Mechanics and Foundation Engineering*, Florence, Italy, Vol. 1, pp. 297-300

Brinkgreve, R.B.J., Broere, W. and Waterman, D. (2004): *PLAXIS 2-D Professional Version 8.0 – User's Manual*, PLAXIS b.v., The Netherlands.

Burd, H.J., Houlsby, G.T., Augarde, C.E. and Liu, G. (2000): 'Modelling tunnelling-induced settlement of masonry buildings', *Proc. Institution of Civil Engineers: Geotechnical Engineering*, 143(1), pp. 17-29

Burland, J.B. and Hancock, R.J.R. (1977).: 'Underground car park at the House of Commons, London: Geotechnical aspects', *Structural Engineer*, 55(2), pp. 81-100

Calvello, M. (2002): *Inverse analysis of supported excavations through Chicago glacial clays*, PhD Thesis, Northwestern University, Evanston, Illinois, USA.

Calvello, M. and Finno, R.J. (2004): 'Selecting parameters to optimize in model calibration by inverse analysis', *Computers and Geotechnics*, 31(5), pp. 411-425

Clough, G.W. and O'Rourke, T.D. (1990): 'Construction induced movements of in-situ walls', *Proc. ASCE Speciality Conference on Design and Performance of Earth Retaining Structures*, Cornell University, New York, pp. 439-470

De Moor, E.K. (1994): 'An analysis of bored pile/diaphragm wall installation effects', *Géotechnique*, 44(2), pp. 341-347

Eisenstein, Z. and Medeiros, L.V. (1983): 'A deep retaining structure in till and sand – Part II: Performance and analysis', *Canadian Geotechnical Journal*, 20, pp. 131-140.

Finno, R.J., Bryson, L.S. and Calvello, M. (2002): 'Performance of a stiff support system in soft clay', *Journal of Geotechnical and Geoenvironmental Engineering*, ASCE, 128(8), pp. 660-671.

Finno, R.J. and Harahap, I.S. (1991): 'Finite element analysis of HDR-4 excavation', *Journal of Geotechnical Engineering*, 117(10), pp. 1590-1609

Hashash, Y.M.A and Whittle, A.J. (1996): 'Ground movement prediction for deep excavations in soft clay', *Journal of Geotechnical Engineering*, ASCE, 122(6), pp. 474-486

Long, M. (2001): 'A case history of a deep basement in London Clay', *Computers and Geotechnics*, 28, pp. 397-423

Mana, A.I. and Clough, G.W. (1981): 'Prediction of Movements for Braced Cut in Clay', *Journal of Geotechnical Engineering*, ASCE, 107(8), pp. 759-777

Moormann, C. and Katzenbach, R. (2002): 'Three-dimensional effects of deep excavations with rectangular shape', *Proc. 2nd International Conference on Soil Structure Interaction in Urban Civil Engineering*, Zurich, Switzerland, Vol. 1, pp. 135-142

Ng, C.W.W. and Lings, M.L. (2002): 'Effects of modelling soil non-linearity and wall installation on back analysis of deep excavation in stiff clay', *Journal of Geotechnical and Geoenvironmental Engineering*, 121(10), pp. 687 - 695

Palmer, J.H.L. and Kenney, T.C. (1972): 'Analytical study of a braced excavation in weak clay', *Canadian Geotechnical Journal*, 9, pp. 145-164

Peck, R.B. (1969a): 'Advantages and limitations of the Observational Method in applied soil mechanics', *Géotechnique*, 19(2), pp. 171-187

Peck, R.B. (1969b): 'Deep excavations and tunnelling in soft ground', *Proc. 7th International Conference on Soil Mechanics and Foundation Engineering*, Mexico, Vol. 3, pp. 225-290

Peck, R.B. (1985): 'The last sixty years', *Proc. 11th International Conference on Soil Mechanics and Foundation Engineering*, San Francisco, pp. 123-133

Powrie, W. and Li, E.S.F. (1991): 'Finite element analyses of an in-situ wall propped at formation level', *Géotechnique*, 41(4), pp. 499-514

Roboski, J.F. (2001): *Soil Parameters for Constitutive Models of Compressible Chicago Glacial Clays*, M.Sc. Thesis, Northwestern University, Evanston, Illinois, USA.

Simpson, B. (1992): 'Retaining structures: Displacement and design', *Géotechnique*, 42(4), pp. 541-576

Wong, K.S. and Broms, B.B. (1989): 'Lateral wall deflections of braced excavation in clays', *Journal of Geotechnical Engineering*, ASCE, 115(6), pp. 853-870